Reprinted from *Earthquake Source Mechanics*
Geophysical Monograph 37 (Maurice Ewing 6)

Published in 1986 by the American Geophysical Union.

THE EFFECT OF FINITE BANDWIDTH ON SEISMIC SCALING RELATIONSHIPS

D. M. Boore

U. S. Geological Survey, Menlo Park, California 94025

Abstract. A breakdown of similarity is generally observed in earthquake sequences below a magnitude of about 5. Although usually manifested as an upper limit on observed corner frequencies (and therefore a decrease of calculated stress drop with decreasing moment), the apparent breakdown can also be seen as changes in the slope of various peak motions plotted against moment. This effect can be explained by a moment-independent high-frequency limit on the band of the recorded signal without specifying whether the limit is imposed by the source, the propagation path, the local site, or the recording instrument. With such a limit, the logarithm of peak acceleration, peak velocity, peak displacement, response spectra, apparent stress, and stress drop will scale for small earthquakes as $1.0 \log M_0$, in contrast to the lesser dependence on moment exhibited for larger earthquakes. The particular filter used in this paper to produce the high-frequency band limitation had the form $\exp(-\pi\kappa f)$, where κ is a parameter controlling the effective corner frequency of the filter. Using an ω-squared, constant-stress-parameter spectral model and a previously published simulation method, I have simulated seismograms for two cases, one for a generic model, with the upper limit to the spectral band spanning a wide range of frequencies, and the other for the aftershock sequence of the 1983 Coalinga, California, earthquake, with κ based on measurements of the spectra. In the first case, the simulations reproduced the general observations with respect to the moment dependence of corner frequencies, stress parameters, and the various measures of peak ground motion. In the second case, the simulations are consistent with the observed seismic-moment scaling of the peak accelerations and peak velocities, for both P and S waves.

Introduction

A pervasive finding of studies of recordings from suites of earthquakes is a breakdown in similarity for earthquakes with magnitudes less than about 5. This breakdown is usually seen as an upper limit to the observed corner frequency and consequently a derived stress drop that decreases with earthquake size. Besides those studies referenced in McGarr [this volume], an apparent breakdown in similarity is also found by Bakun et al. [1976], Rautian et al. [1978], Fletcher [1982], Nuttli [1983], Scherbaum and Stoll [1983], Haar et al. [1984], Scherbaum and Kisslinger [1984], I. Apopei [personal communication, 1985], and A. Rovelli [personal communication, 1985], among others. The earthquakes studied in the referenced papers occurred in California, Alaska, South Carolina, Arkansas, Missouri, Tadjikistan (USSR), Italy, Romania, and Germany. Another manifestation of this apparent breakdown in similarity is the divergence of the scaling of peak acceleration and velocity from that expected from theoretical arguments based on source spectra obeying the similarity conditions [McGarr et al., 1986; McGarr, this volume].

This nonsimilar behavior has been interpreted widely as a source effect (involving either an upper limit to the frequency radiated or a dependence of stress on moment). The purpose of this paper is to explore the possibility that the effect could be explained by any process that limits high frequencies, whether it be due to the instrument, source, or site. Others have remarked on the influence of the bandwidth on observed ground motions and derived source parameters [e.g., Hanks, 1982; Hanks and McGuire, 1981; Hanks and Boore, 1984]. This paper presents a more comprehensive and quantitative investigation of the effects than has been previously published.

Method

Although the apparent divergence from similarity has most often been seen in plots of seismic moment versus corner frequency or stress drop, the emphasis in this paper will be on the scaling of peak velocity (v_p) and acceleration (a_p) on seismic moment, as the effect of a finite bandwidth is less obvious for these measures than it is for stress drop. Hanks [1982] has discussed the implications of a moment-independent bandwidth on stress drop.

The approach is to derive theoretical estimates of v_p and a_p corresponding to a spectral model of the radiated energy that includes a moment-independent low-pass filter. The method for deriving theoretical estimates of v_p and a_p has been presented before [Boore, 1983]; it basically consists of filtering a time series made up of windowed, white Gaussian noise. It might seem that the method, being based on a stochastic series, might be inapplicable for the simula-

TABLE 1. Amplification Factors for P and S Waves

Frequency (Hz)	δ (P waves)*	δ (S waves)*
0.10	0.01	0.01
0.32	0.04	0.04
1.	0.13	0.13
3.2	0.17	0.34
10.	0.19	0.37

From Boore [1986].
*Amplification $= 10^{\delta}$.

tion of the simple pulselike waveforms often characterizing records from small events. This, however, is not the case. The simulated ground motion can be simple or complex in appearance, depending on the filter parameters [Boore, 1983, Figure 5]. The spectrum of the motion used in the filtering of the random time series was taken to be:

$$R(f) = C(2\pi f)^n S(f) A(f) D(f) \qquad (1)$$

where the power n determines whether the velocity ($n = 1$) or acceleration ($n = 2$) is being considered. The factors C, $S(f)$, $A(f)$, and $D(f)$ stand for a scaling factor, the source spectrum, an amplification factor, and diminution factor, respectively. Only $S(f)$ depends on the seismic moment. C was given by

$$C = \frac{\langle R_{\Theta\Phi}\rangle F V}{4\pi\rho_s c_s^3}\left(\frac{1}{r}\right) \qquad (2)$$

where $\langle R_{\Theta\Phi}\rangle$ is an average of the radiation pattern, F is included to account for free-surface effects, V represents the partition of a vector into horizontal components (in some cases this is absorbed into $\langle R_{\Theta\Phi}\rangle$), ρ_s and c_s are the density and seismic velocity in the vicinity of the source, and r is the distance from the source to the point of estimation. A standard ω-square model was used:

$$S(f) = M_0 / \left[1 + (f/f_0)^2\right] \qquad (3)$$

M_0, the static seismic moment, and f_0, the corner frequency, were related through a parameter, $\Delta\sigma$, having dimensions of stress, according to the following formula adapted from Boore [1983]:

$$f_0 = 4.9 \times 10^4 \beta \lambda \left(\Delta\sigma / M_0\right)^{1/3} \qquad (4)$$

where β is the shear velocity in km/s and, for P-waves, λ is the ratio of the P and S corner frequencies. The units of $\Delta\sigma$ and M_0 are MPa and N m, respectively. It is important to distinguish the stress quantity $\Delta\sigma$, used as a parameter in the theoretical calculations, from the stress drop derived from measurements of long period spectral level and corner frequency; as will be shown (and Hanks [1982] has pointed out), high-frequency filtering effects can obscure the source corner frequency f_0.

The amplification filter $A(f)$ can take various forms. It is included in an attempt to account for the relatively broadband amplification expected for any propagation upward through the progressively slower velocity materials usually found in the upper few kilometers of the crust. The details are contained in Boore [1986], and the amplification factors are given in Table 1. Briefly, the amplification is given by the square root of the ratio of the seismic velocity near the source and the near-surface velocity. An effective velocity over a quarter wavelength is used for the latter, thus making the amplification dependent on frequency. This amplification is in addition to the resonant amplification that would be produced by strong impedance contrasts; resonant amplification is not included in this study.

The final term in (1) represents the bandwidth limitation, whose influence is the subject of this paper. A useful form of this filter is

$$D(f) = \exp(-\pi f r / Q(f) c) \exp(-\pi\kappa f) \qquad (5)$$

The first term represents the attenuation in propagating a distance r and the second term is a distance-independent low-pass filter. The latter term is of the form proposed by Anderson and Hough [1984], although they allow the coefficient in front of the frequency to be a function of distance; at the risk of some confusion in terminology, I have taken κ to be independent of distance. A possible physical mechanism for the second term would be near-site attenuation in the last few kilometers of the ray path. For small distances or large Q, the second term contributes most of the attenuation and the effect of the filter $D(f)$ on peak velocity and acceleration is then roughly equivalent to a step high-cut filter with cutoff frequency (f_{max}) equal to $1/\pi\kappa$ (a relation pointed out to me by J. Boatwright and subsequently confirmed by my simulations).

Results

A suite of spectra derived from (1) are shown in Figure 1. The parameters have been chosen so as to make these spectra similar to those of Anderson [this volume]. With the reasonable assumption that peak motions are proportional to the maximum spectral amplitudes, the following qualitative conclusions about the scaling of the peak motions can be drawn without complex calculations, simply from the spectral shapes and the spacing between the spectral maxima: for large earthquakes, the peak velocity will be a stronger function of seismic moment (or, equivalently, moment magnitude) than will peak acceleration. In contrast, the moment dependence of both peak acceleration and peak velocity will be identical for small earthquakes and will have a stronger dependence on moment than do either a_p and v_p for large earthquakes.

Quantitative analysis of the expected scaling gives

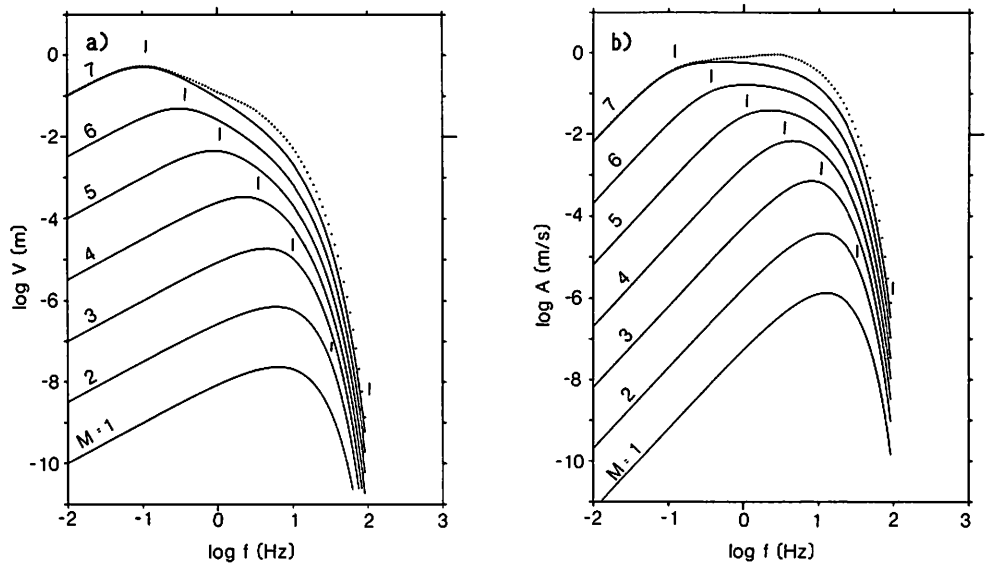

Fig. 1. Velocity and acceleration spectra for a range of moment magnitudes, computed for $r = 10$ km, $\rho_s = 2.7$ gm/cc, $c_s = 3.2$ km/s, $\langle R_{\Theta\Phi} \rangle = 0.5$, $F = 1.0$, $V = 1.0$, $\kappa = 0.05$, and a stress parameter of 10 MPa (see equations (1) through (4) for meaning of terms). The vertical bars indicate corner frequencies, computed from equation (5) in Boore [1983]. Dots show modification of $M = 7$ spectra for amplification factors given in Table 1.

$$\log v_p \propto 0.37 \log M_0 \tag{6a}$$

and

$$\log a_p \propto 0.20 \log M_0 \tag{6b}$$

for large M_0 (Boore [1983]; for a different model, McGarr [1984] gives $\log v_p \propto 0.33 \log M_0$ and $\log a_p \propto 0.0 \log M_0$). For small events, the scaling is

$$\log v_p \propto 1.0 \log M_0 \tag{7a}$$

and

$$\log a_p \propto 1.0 \log M_0 \tag{7b}$$

The scaling for small M_0 is a direct consequence of the upper limit on the bandwidth. If frequencies are not present above a cutoff which is small compared to the reciprocal source duration, then the seismic record will be a simple impulse response with amplitude proportional to M_0. The time series for any particular type of ground motion or instrument type will have the same shape independent of M_0 and the amplitude will be proportional to M_0. In particular, the logarithms of the peak response of a Wood-Anderson instrument (and thus M_L), the peak ground displacement and the peak response spectra will scale the same way as do v_p and a_p in (7); radiated energy will scale as $M_0^{2.0}$. Therefore, the presence of a bandwidth limiting effect, due to instrument response or source- or site-processes, can produce significant differences in the expected scaling of peak motions for large and small earthquakes. It is also clear from comparing the specified corner frequencies (vertical bars in Figure 1) with the spectra that observed corner frequencies for small earthquakes will be constant, in apparent violation of the constant stress drop model used in deriving the results. Because derived stress drop is proportional to the product of moment and the cube of corner frequency, the derived stress drop will scale as $M_0^{1.0}$, just as do v_p and a_p.

The scaling results given above only apply for very large and very small earthquakes. I have made a more complete analysis by simulating the acceleration and velocity time series using the method of Boore [1983]. Peak acceleration, velocity, and apparent stress have been derived from the geometrical mean of the corresponding quantities, for ensembles of 100 simulations. Two models have been considered. The first uses the same stress and κ parameters used by Anderson [this volume] in investigating the moment dependence of the frequency characterizing the upper end of the spectral bandwidth. (This frequency was named f_{95} by Anderson and is similar in effect and meaning to Hanks' $f_{\max}$ [Hanks, 1982]). My results thus complement his by considering the influence of finite bandwidth on observational quantities other than f_{95}. A second model is specific to the data set from the 1983 Coalinga, California, earthquake sequence. This sequence was well recorded on portable, high-dynamic-range, digital-recording portable instruments [Mueller et al., 1984] and provides an excellent data set for studying the scaling of ground motion for small to moderate events.

For the first model, the scaling of v_p and a_p from S waves confirms the earlier predictions based on examina-

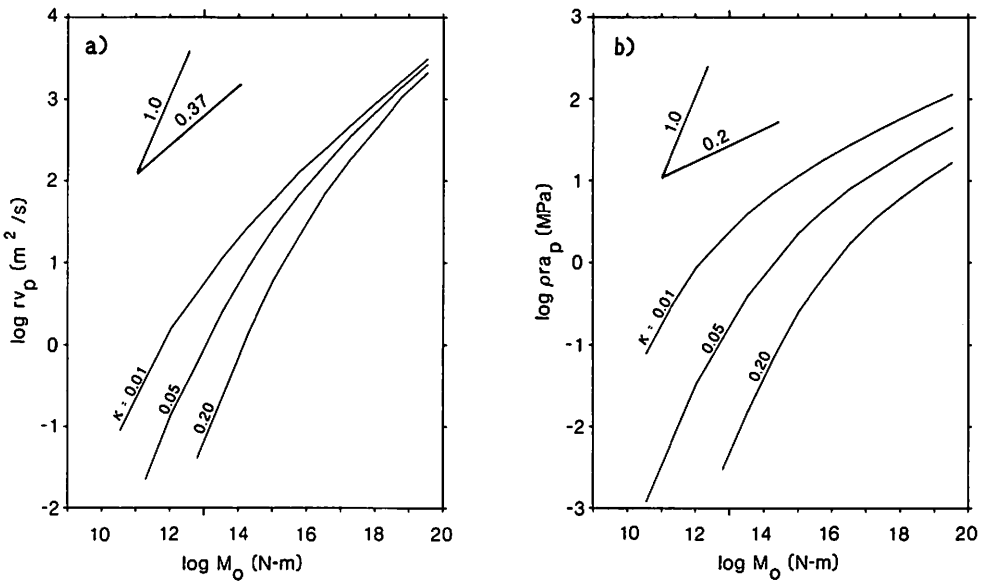

Fig. 2. Peak velocity and acceleration, corrected for geometrical spreading, as a function of moment for values of κ used by Anderson [this volume]. Other parameters given in caption to Figure 1. Short lines show expected scaling for earthquakes with large and small seismic moments (equations (6) and (7)).

tion of the spectra (Figure 2). The transition between the different slopes is a function of the parameter κ. If thought of as representing anelastic attenuation (i.e., $\kappa = t/Qc$), $\kappa = 0.01$, and $\kappa = 0.20$ correspond to small and large attenuation, respectively [Anderson, this volume]. $\kappa = 0.05$ is an average value for weathered rock. Recordings of aftershock sequences using portable digital instruments are usually dominated by earthquakes in the 10^{11} to 10^{16} N-m (10^{18} to 10^{23} dyne-cm) range of seismic moment, and thus Figure 2 indicates that the source systematics derived from such recordings can be strongly influenced by finite bandwidth effects.

Another quantity computed from seismic observation is the apparent stress, defined as:

$$\sigma_a = \mu E_s / M_0 \qquad (8)$$

where μ is the rigidity and E_s is the radiated seismic energy. This quantity has been computed for the first model. Time domain velocities were integrated to derive energy, and a correction was applied to account for whole-path attenuation at the frequency of the peaks in the velocity spectra. The results show a pronounced dependence of apparent stress on moment, with an abrupt transition to an approximately constant level (Figure 3). The slope of $\log \sigma_a$ vs $\log M_0$ is unity for small earthquakes, in perfect agreement with the expectation from (1) and (3), when Parseval's theorem is used to relate the time domain and frequency domain estimates of energy. Observational studies of the 1976 Friuli earthquake in Italy (A. Rovelli, personal communication, 1985) and the 1983 Coalinga, California, earthquake (M. Andrews, personal communication, 1985) are in agreement with the expected slope, although the σ_a values for the latter earthquake show considerable scatter.

The results in Figures 2 and 3 are for a generic model,

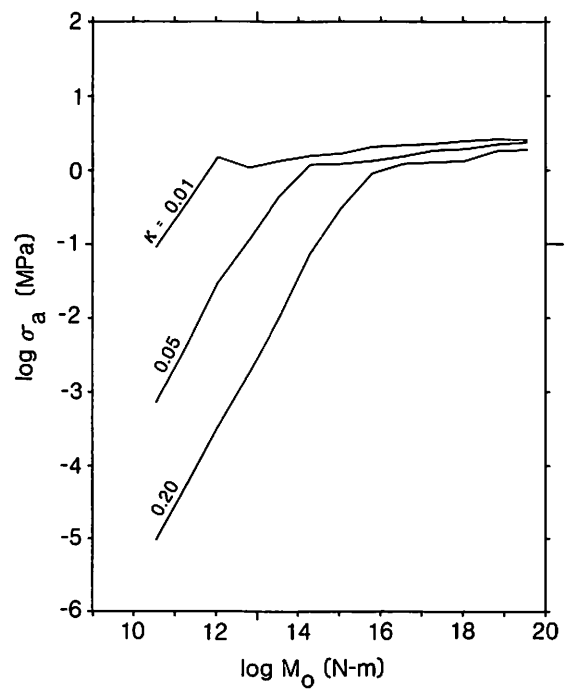

Fig. 3. Moment dependence of apparent stress for model used in Figures 1 and 2.

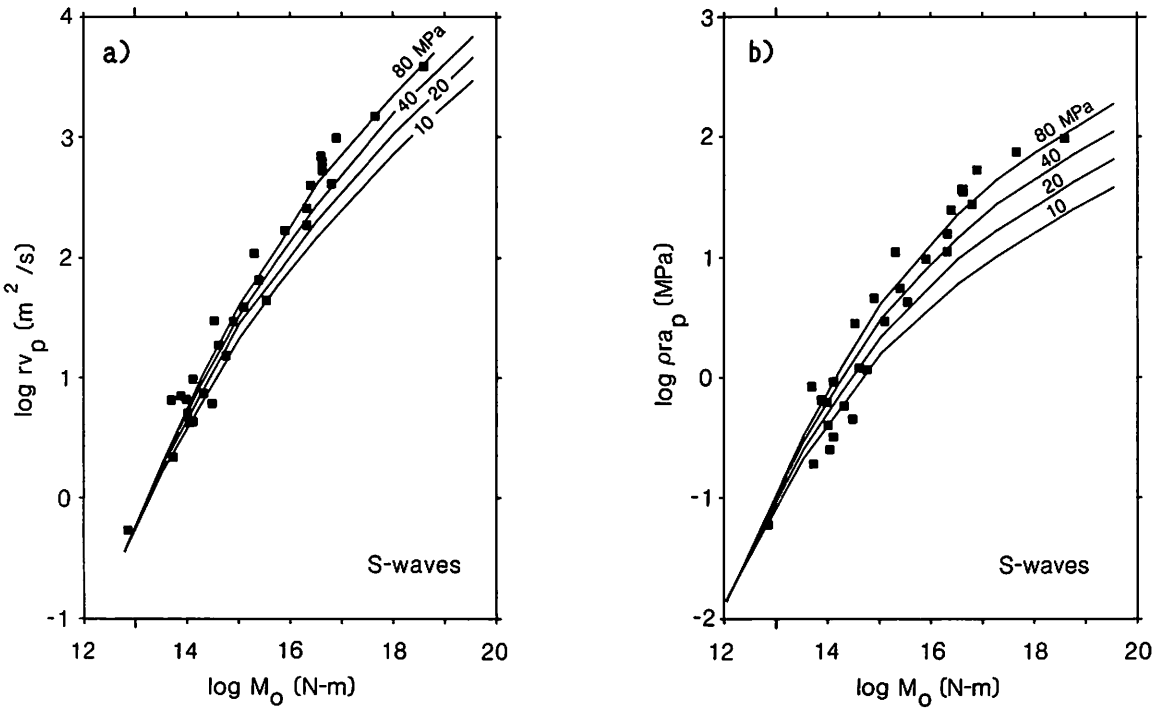

Fig. 4. Observed (squares) and predicted (lines) velocities and accelerations for S waves from 1983 Coalinga, California, earthquake sequence. Data from McGarr et al. [1986]. Theoretical calculations used $Q(f)$ given by equation (6) in Boore [1984], $\kappa = 0.07$, $\langle R_{\Theta\Phi} \rangle = 0.6$, $F = 1.0$, $V = 1.0$, $\rho_s = 2.7$ gm/cm^3, $c_s = 3.2$ km/s, and $\Delta\sigma$ ranging from 10 to 80 MPa. No amplification was included.

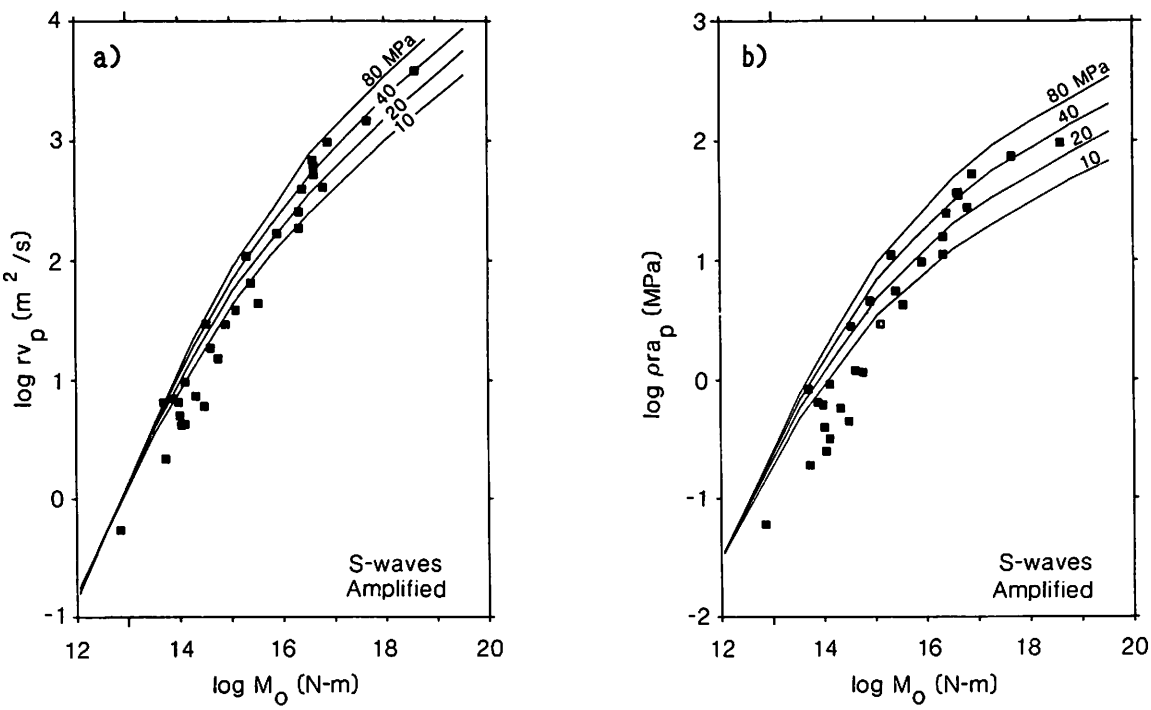

Fig. 5. S wave observations and predictions (using amplifications in Table 1). See Figure 4 for other parameters.

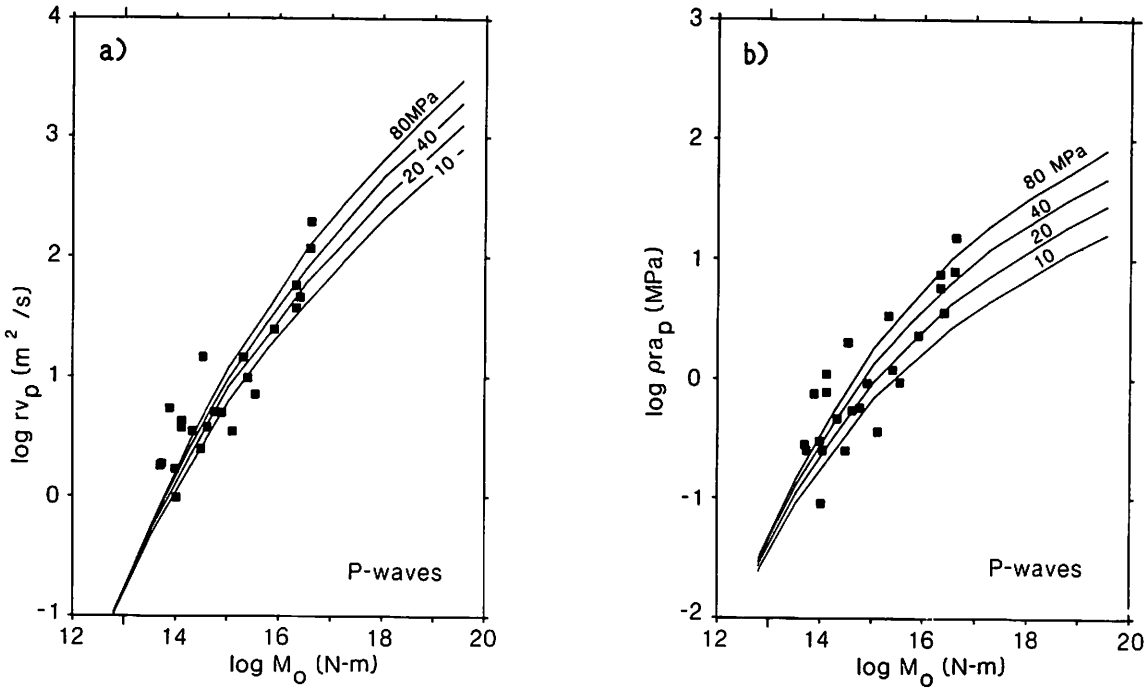

Fig. 6. The same as Figure 4, but for P rather than S waves and $\kappa = 0.047$, $c_s = 5.5$ km/s, $\langle R_{\Theta\Phi} \rangle = 0.36$, and the P corner frequency equal to 1.5 times the S corner frequency. Amplification has not been included.

chosen to be consistent with that considered by Anderson [this volume] and intended to illustrate the general effects expected from bandwidth limitations. The second application is specific to the data collected from the 1983 Coalinga, California, earthquake sequence. McGarr et al. [1986] have measured a_p and v_p using records from portable digital seismographs and analog accelerographs. Most of the earthquakes were recorded at a number of sites, with the digital instruments providing the bulk of the data. Accelerograph recordings at one station were used for the mainshock. McGarr et al. [1986] removed the free-surface effect and combined the components vectorially to yield the peak motion. They reduced the measurements to unit distance by multiplying v_p and a_p by r and $\rho_s r$, respectively. An attempt was made to maximize the values of rv_p averaged over the suite of recordings of any one earthquake, using a similar part of the waveform at all stations; consequently, the v_p used may not correspond to the actual peak motions on any one seismogram. This should be kept in mind when comparing the observations with the theoretical calculations, which represent the peak value of motions from a point source.

To permit comparison with the results of McGarr et al. [1986] and McGarr [this volume], the free-surface effect was ignored ($F = 1$). Furthermore, McGarr and colleagues consider vector motion, so V was set to unity. Following Boore and Boatwright [1984], the value of $\langle R_{\Theta\Phi} \rangle$ was derived from an average of the logarithm of the radiation pattern of the total S- and P-wave motion at close distances from a buried dip-slip source ($\langle R_{\Theta\Phi} \rangle = 0.6$ and $\langle R_{\Theta\Phi} \rangle = 0.36$ for S and P waves, respectively). The value of κ used in the calculations of the S-wave motions was a rough average of values measured by M. Andrews (personal communication, 1985) from acceleration spectra for a set of Coalinga data that overlaps, but is not identical to, the earthquake/station pairs providing McGarr et al.'s [1986] a_p and v_p data. Using the method of Anderson and Hough [1984], Andrews' estimates were based on fitting a straight line, in the range of frequencies from about 5 to 20 Hz, to log-linear plots of the spectra. The limited distance range and the large scatter precluded finding a dependence of κ on distance.

A comparison of observations and theory, without amplification, is given in Figure 4. A range of stress parameters, $\Delta\sigma$, from 10 to 80 MPa was used. As expected, $\Delta\sigma$ has little effect on the motions of small earthquakes, whose spectral amplitudes are a function of M_0 only (e.g., Figure 1). As seen in Figure 2, the effect of κ is complementary to that of $\Delta\sigma$, for it has more influence on small earthquakes than large events.

A comparison of the normalized a_p and v_p data shows that although they both have a similar trend for small earthquakes (with a slope close to unity), the dependence on seismic moment is different for large earthquakes, with v_p being a stronger function of M_0 than is a_p. This corresponds directly to the theoretical expectations expressed

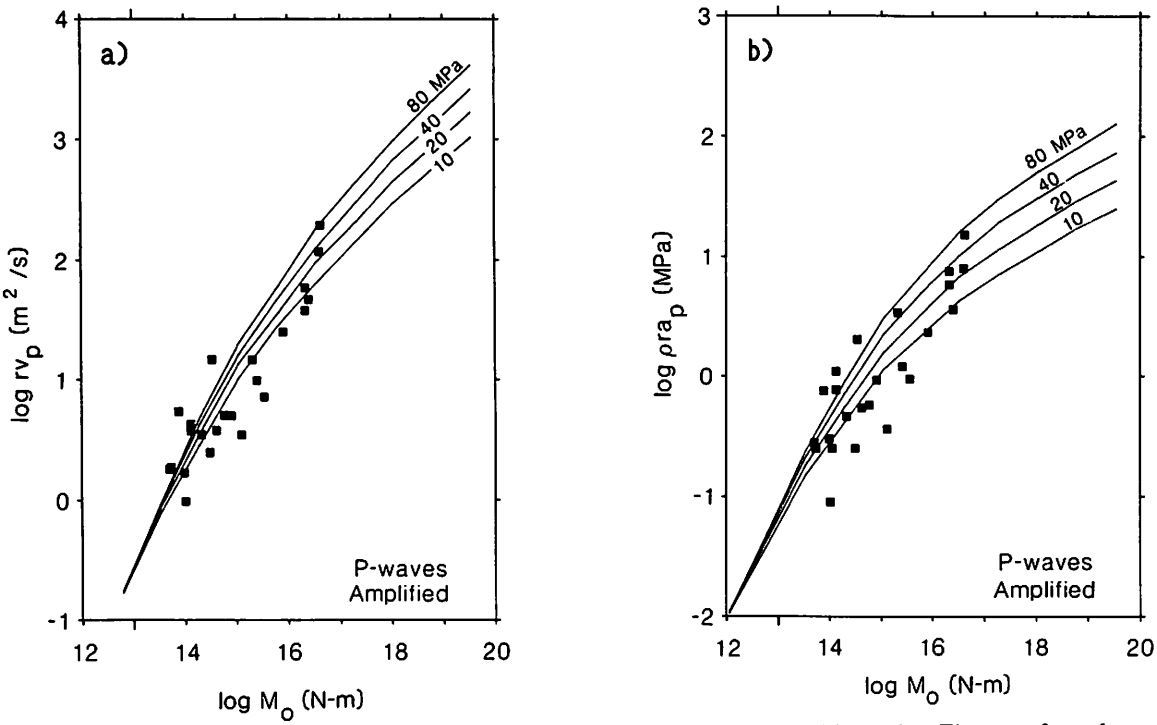

Fig. 7. *P* wave observations and predictions, using amplifications in Table 1. See Figure 6 for other parameters.

in (6) and (7). The fits to the absolute values are not bad for the smaller earthquakes, but for the large earthquakes the theory requires $\Delta\sigma$ close to 80 MPa. Including amplification makes it possible to fit the data with $\Delta\sigma \approx 30$ MPa, a high but not unreasonable value (Figure 5). The amplification factors used in the calculations are for motions on the highly fractured rock typical of much of California; for soil sites the amplification could be as much as a factor of two larger. Since a number of the Coalinga recordings were obtained on sites underlain by soil, it is possible that the amplification factors could be larger than in Table 1, thus leading to a stress parameter less than 30 MPa. With amplification, the data for smaller earthquakes do not fit the theory as well as they did without amplification, but there is a consistent explanation for this: the moments used for the data were measured without correcting for amplification. If amplification exists, the moments derived for the data should be decreased, and if the amplification is due to propagation through a near-surface velocity gradient, the correction should be larger for small earthquakes than for large earthquakes (see, e.g., the solid and dashed curves in Figure 1). According to Table 1, this correction could amount to over 0.3 log units for the smaller earthquakes.

The measurements of *P* wave amplitudes from the Coalinga earthquake recordings provide another opportunity to compare the predicted effect of finite bandwidth with observations. Comparisons of predicted and observed peak motions, without and with amplification, are given in Figures 6 and 7, respectively. As with the *S* waves, the comparison is good, both in trend and absolute amplitude. In making the predictions, the ratio of *P* and *S* corner frequencies was taken to be 1.5, following the observations of McGarr et al. [1986]. The ratio of κ was also assumed to be 1.5, with κ smaller for *P* waves. The amplification factors given in Table 1 were used in the calculations.

Conclusions

A moment-independent filter that attenuates high frequencies produces marked changes in the scaling expected from the usual analysis of self-similar models. For small earthquakes many quantities derived from the ground motion will scale directly with the seismic moment, even though for large earthquakes the quantities might depend weakly, if at all, on seismic moment. Examples of quantities scaling linearly with moment include stress drop, apparent stress, peak displacement, peak acceleration, peak velocity, and peak response of a Wood-Anderson instrument. These conclusions are important because earthquakes in the moment range expected to be affected by bandwidth limitations are numerous (particularly in aftershock sequences) and are often recorded. Most studies of such events have found the type of effects predicted here, but have usually attributed them to a breakdown in the self-similarity of the earthquake source. Of course, I have not shown that the source is not the ultimate cause of

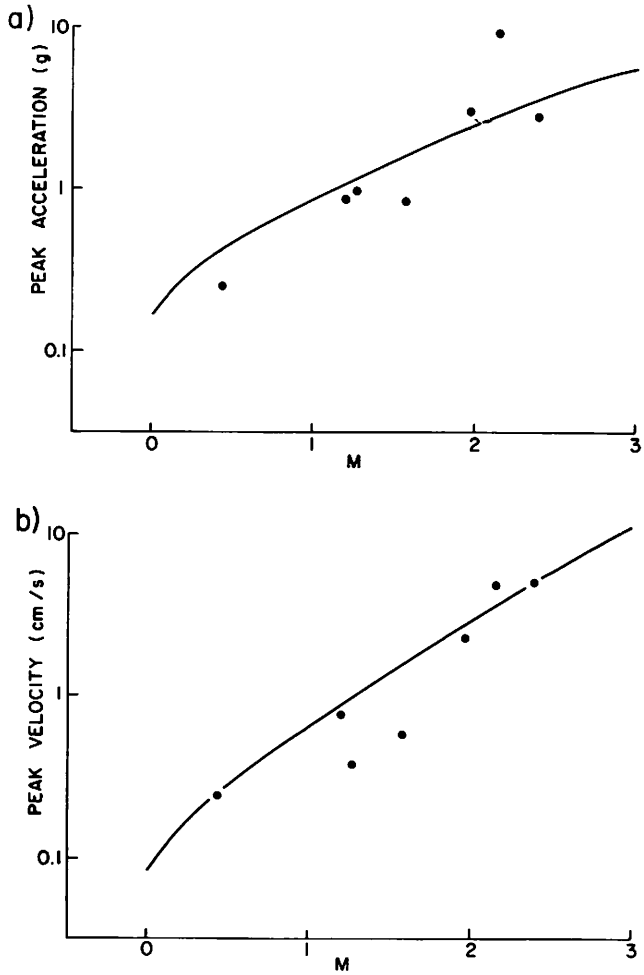

Fig. 8. Comparison of peak accelerations and velocities from South African accelerograms (figure from Boore [1983]). Data: dots, theory: lines. Calculations at 200 m, using $c_s = 3.8$ km/s, $Q(f) = 600$, $\Delta\sigma = 5$ MPa, and a high-frequency cutoff of 400 Hz.

the band limitation. I have simply investigated the consequences of such a high-frequency filter, regardless of its origin. The origin cannot be neglected, however, for whether or not high-frequency waves are radiated from the source can have important consequences for the design of structures. If high-frequency waves are radiated from the source and are attenuated in the vicinity of the recording site, then a study of the attenuation characteristics of proposed sites would be an important aspect of planning short-period structures. If high-frequency waves are not radiated from the source, then such a study is not necessary. Although it is reasonable to expect attenuation during wave propagation through the material near the earth's surface (even on rock sites), a definitive study of the causes of the removal of high frequencies from the radiated field will require recordings at varying depths in the earth and at a variety of surface sites for a suite of earthquakes.

The results of peak-velocity scaling for a number of earthquake sequences, summarized by McGarr [this volume], are roughly consistent with the prediction from Figure 2 that the more competent the rock near the recording site, the lower the moment at which the transition in scaling takes place. The extremes in McGarr's data correspond to the Coalinga and the mine-tremor data, recorded on soils and incompetent rock in the first case and very sound rock in the second. The Mirimichi, New Brunswick, data are from sites that fall between these extremes. I have considered the Coalinga data in this paper and in an earlier paper [Boore, 1983] showed that a standard ω-square, constant-stress-parameter model could simultaneously explain both the peak accelerations and the peak velocities from the deep-mine tremors, using a high-frequency filter appropriate for the recording site. This is shown in Figure 8 (fewer data were available for that study than are presented in McGarr). These quantitative comparisons, as well as the general trends of the transition moments in McGarr [this volume], suggest that near-site attenuation plays an important role in the observed scaling.

Acknowledgments. I thank Mary Andrews, William Joyner, and Art McGarr of the U.S. Geological Survey for stimulating discussions and Ezio Faccioli, Charles Mueller, Antonio Rovelli, and Frank Scherbaum for thoughtful reviews. This research was partially supported by a grant from the U.S. Nuclear Regulatory Commission.

References

Anderson, J. G., Implication of attenuation for studies of the earthquake source, this volume, 1986.

Anderson, J. G., and S. E. Hough, A model for the shape of the Fourier amplitude spectrum of acceleration at high frequencies, Bull. Seismol. Soc. Am., 74, 1969–1993, 1984.

Bakun, W. H., C. G. Bufe, and R. M. Stewart, Body-wave spectra of central California earthquakes, Bull. Seismol. Soc. Am., 66, 363–384, 1976.

Boore, D. M., Stochastic simulation of high-frequency ground motions based on seismological models of the radiated spectra, Bull. Seismol. Soc. Am., 73, 1865–1894, 1983.

Boore, D. M., Use of seismoscope records to determine M_L and peak velocities, Bull. Seismol. Soc. Am., 74, 315–324, 1984.

Boore, D. M., Short-period P- and S-wave radiation from large earthquakes: implications for spectral scaling relations, Bull. Seismol. Soc. Am., 76, 43–64, 1986.

Boore, D. M., and J. Boatwright, Average body-wave radiation coefficients, Bull. Seismol. Soc. Am., 74, 1615–1621, 1984.

Fletcher, J. B., A comparison between tectonic stress measured in situ and stress parameters from induced seismicity at Monticello Reservoir, South Carolina, J. Geophys. Res., 87, 6931–6944, 1982.

Haar, L. C., J. B. Fletcher, and C. S. Mueller, The 1982 Enola, Arkansas, swarm and scaling of ground motion in

the eastern United States, Bull. Seismol. Soc. Am., 74, 2463–2482, 1984.

Hanks, T. C., f_{max}, Bull. Seismol. Soc. Am., 72, 1867–1879, 1982.

Hanks, T. C., and D. M. Boore, Moment-magnitude relations in theory and practice, J. Geophys. Res., 89, 6229–6235, 1984.

Hanks, T. C., and R. K. McGuire, The character of high-frequency strong ground motion, Bull. Seismol. Soc. Am, 71, 2071–2095, 1981.

McGarr, A., Scaling of ground motion parameters, state of stress, and focal depth, J. Geophys. Res., 89, 6969–6979, 1984.

McGarr, A., Some observations indicating complications in the nature of earthquake scaling, this volume, 1986.

McGarr, A., C. Mueller, J. B. Fletcher, and M. Andrews, Ground motion and source parameters of the 1983 Coalinga, California earthquake sequence, in The Coalinga, California, earthquake sequence of May 2, 1983, U.S. Geol. Surv. Prof. Pap., in press, 1986.

Mueller, C. S., E. Sembera, and L. Wennerberg, Digital recordings of aftershocks of the May 2, 1983 Coalinga, California earthquake, U.S. Geol. Surv. Open-File Rep., 84-697, 57 pp., 1984.

Nuttli, O. W., Average seismic source-parameter relations for mid-plate earthquakes, Bull. Seismol. Soc. Am., 73, 519–535, 1983.

Rautian, T. G., V. I. Khalturin, V. G. Martynov, and P. Molnar, Preliminary analysis of the spectral content of P and S waves from local earthquakes in the Garm, Tadjikistan region, Bull. Seismol. Soc. Am., 68, 949–971, 1978.

Scherbaum, F., and C. Kisslinger, Variations of apparent stresses and stress drops prior to the earthquake of 6 May 1984 ($m_b = 5.8$) in the Adak seismic zone, Bull. Seismol. Soc. Am., 74, 2577–2592, 1984.

Scherbaum, F., and D. Stoll, Source parameters and scaling laws of the 1978 Swabian Jura (southwest Germany) aftershocks, Bull. Seismol. Soc. Am., 73, 1321–1343, 1983.